Bulletin of the Earthquake
Research Institute
Vol. 53 (1978), pp. 359-378

14. Characteristics of Elasto-Plastic Ground Motion During an Earthquake.

By Yozo Fujino,
Institute of Structural Engineering,
University of Tsukuba

and

Motohiko Hakuno,
Earthquake Research Institute.

(Received April 28, 1978.)

1. Introduction

The stress-strain relation of soil material generally reveals nonlinearity when its strain exceeds $10^{-4}\sim10^{-3}$. In ground motions due to earthquakes of small and medium size, the nonlinear effect of soil would be practically negligible, since the maximum strain of the soil hardly exceeds 10^{-3}. However, during strong earthquakes the mechanical behavior of the soil is nonlinear to a considerable extent, resulting in nonlinear ground motions. This is evident from the observation that railways and roads have occasionally undergone permanent deformation due to the ground motions of strong earthquakes. Unfortunately, the record of such a strong earthquake on the ground has not been obtained so far. Therefore, many studies concerning linear or nonlinear ground motion have been made to find the ground motion characteristics of strong earthquakes. Methods of analysis to obtain the earthquake response of the ground can be categorized into two groups: one is an analytical method based on wave propagation theory, the other the matrix method, the so-called Finite Element Method (FEM).

The first method has been developed and applied to various problems of ground motions by Kanai (1932) and others. They have found certain ground motion characteristics, for example, the existence of a predominant period of the ground. However, this method entails certain difficulties if we wish to consider nonlinearity of the soil material and to solve complex boundary condition problems. On the other hand, the second method is effective with respect to the two above-mentioned problems. Above all, it is one of the most effective methods for studying the dynamic interaction of a structure and the surrounding ground. Many papers on elastic or elasto-plastic dynamic analysis by FEM have been written (Seed and Idriss, 1970). However, it should be mentioned that the dynamic analysis

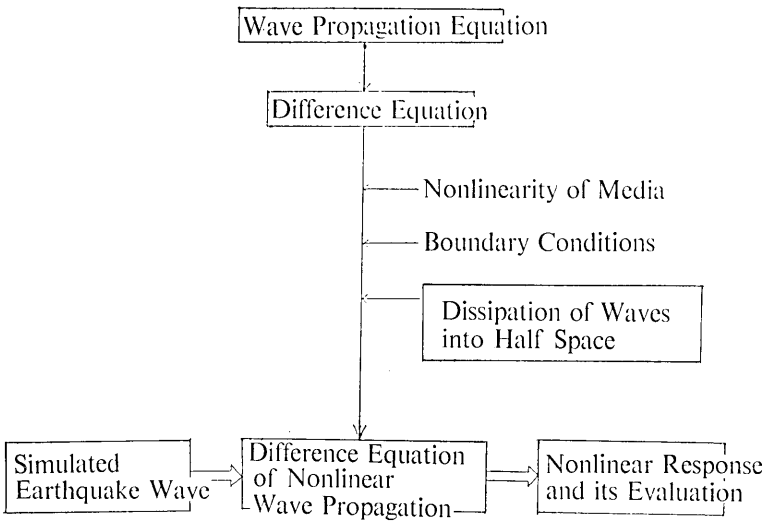

Fig. 1. Flowchart of analysis.

of the ground by FEM has not succeeded in rigorously treating earthquake waves dissipating into an infinite half-space, which is one shortcoming.

In this paper, following the work made by OKAMOTO and HAKUNO (1962), a difference equation, including the effects of the nonlinearity of the soil and the dissipating wave energy, is derived from the one-dimensional wave equation (Figure 1). In a ground model which consists of two layers, we will examine, by means of the derived difference equation, how the nonlinear dynamic response of the ground during a strong earthquake differs from the linear response, especially with respect to the following two points:

1) Predominant period

In general, the existence of the predominant period of the ground has been confirmed theoretically and also from observation. We wish to know how the predominat period will change during a strong earthquake due to the nonlinearity of the soil material.

2) Amplification factor of a surface layer

In the elasto-plastic response of a structural system such as a steel member, it is generally recognized that the stress-strain curve of the system draws a hysteresis loop and that this consumes vibrational energy. Therefore, the nonlinear response does not increase in proportion to the magnitude of the excitation. The question arises whether there is such a characteristic in nonlinear ground motion.

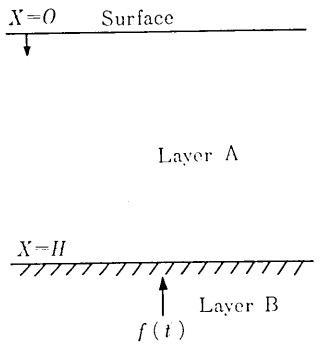

Fig. 2. Ground model.

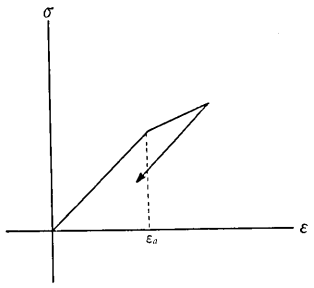

Fig. 3. Assumed stress-strain gurve.

2. Modelling of the ground

A soft ground layer A overlying a half-space B, as shown in Figure 2, is adopted as the ground model in this analysis. Incident waves are assumed to propagate upwards vertically to the surface layer A. Since shear waves are considered to play a major role in causing damage to soil foundations and structures, the following shear wave equation can be used in the analysis.

$$\rho\frac{\partial^2 U}{\partial t^2}=\frac{\partial \sigma}{\partial x} \tag{1}$$

where

U=horizontal displacement of the ground
ρ=density of the ground soil
t=time
σ=shear stress
x=co-ordinate in the depth direction.

Note that (1) holds when the soil is not only in elastic state, but also in the elasto-plastic state, since it is derived from the equilibrium of forces.

It is assumed that the stress-strain relation of the soil in the layer A is of a bi-linear type as shown in Figure 3. The shear modulus after yielding is expressed by aG (G=the elastic shear modulus, $0\leq a\leq 1$).

3. Difference equation

In this paper, (1) is solved numerically by the equivalent difference equation which satisfies the boundary conditions of the ground model. Expressing (1) in terms of the difference equation, one obtaines

$$\rho\frac{U_{n,m+1}-2U_{n,m}+U_{n,m-1}}{\Delta t^2}=\frac{\sigma_{n+1}-\sigma_n}{\Delta x} \tag{2}$$

which is equivalent to

$$\begin{aligned}U_{n,m+1}&=\frac{\Delta t^2}{\Delta x}\frac{1}{\rho}(\sigma_{n+1}-\sigma_n)+2U_{n,m}-U_{n,m-1}\\&=\frac{\Delta t^2}{\Delta x}\frac{G}{\rho}(\varepsilon_{e,n+1}+a\varepsilon_{p,n+1}-\varepsilon_{e,n}-\varepsilon_{p,n})\\&\quad+2U_{n,m}-U_{n,m-1}\quad\text{(in layer A)}\end{aligned} \tag{3}$$

$$\begin{aligned}U_{n,m+1}&=\frac{\Delta t^2}{\Delta x}\frac{G}{\rho}(U_{n+1,m}-2U_{n,m}+U_{n-1,m})\\&\quad+2U_{n,m}-U_{n,m+1}\quad\text{(in layer B).}\end{aligned} \tag{4}$$

If one chooses, Δt and Δx so that they satisfy $(G\Delta t^2/\rho\Delta x)=1$, (4) yields

$$U_{n,m+1}=U_{n+1,m}+U_{n-1,m}-U_{n,m-1} \tag{5}$$

where

Δt=time interval
Δx=grid point interval
G=elastic shear modulus
aG=shear modulus after yielding
ε_e=elastic strain
ε_p=plastic strain
m=grid point number indicating time
n=grid point number indicating depth from the surface.

Knowing the values of $U_{n,m}$ and $U_{n,m-1}$, one can calculate the displacement $U_{n,m+1}$ by (3) and (5). The elastic strain ε_e and plastic strain ε_p can be obtained as follows. When the displacements $U_{i,m+1}$ $(i=1, 2, 3, \cdots)$ at the $m+1$ step are obtained, the strain $\varepsilon_{n,m+1}$ is given by

$$\varepsilon_{n,m+1}=\frac{U_{n,m+1}-U_{n-1,m+1}}{\Delta x}. \tag{6}$$

Hence the strain increment $\Delta\varepsilon_{n,m+1}$ with respect to time is expressed as

$$\Delta\varepsilon_{n,m+1}=\varepsilon_{n,m+1}-\varepsilon_{e,n,m}-\varepsilon_{p,n,m}. \tag{7}$$

Using the elastic strain limit ε_a, the elastic strain $\varepsilon_{e,n}$ and plastic strain $\varepsilon_{p,n}$ are obtained as follows.

i) If $|\varepsilon_{e,n,m}|<\varepsilon_a$

a) If $|\varepsilon_{e,n,m}+\Delta\varepsilon_{n,m+1}|<\varepsilon_a$

$$\varepsilon_{e,n,m+1}=\varepsilon_{e,n,m}+\Delta\varepsilon_{n,m+1}$$
$$\varepsilon_{p,n,m+1}=\varepsilon_{p,n,m}$$

b) If $|\varepsilon_{e,n,m}+\Delta\varepsilon_{n,m+1}|>\varepsilon_a$

1) If $\varepsilon_{e,n,m}>0$

$$\varepsilon_{e,n,m+1}=\varepsilon_a$$
$$\varepsilon_{p,n,m+1}=\varepsilon_{p,n,m}+\varepsilon_{e,n,m},+\Delta\varepsilon_{n,m+1}-\varepsilon_a$$

2) If $\varepsilon_{e,n,m}<0$

$$\varepsilon_{e,n,m+1}=-\varepsilon_a$$
$$\varepsilon_{p,n,m+1}=\varepsilon_{p,n,m}-\varepsilon_{e,n,m}-\Delta\varepsilon_{n,m+1}+\varepsilon_a$$

ii) If $|\varepsilon_{e,n,m}|=\varepsilon_a$

a) If $\Delta\varepsilon_{n,m+1}\cdot\varepsilon_{e,n,m}>0$

$$\varepsilon_{e,n,m+1}=\varepsilon_{e,n,m}$$
$$\varepsilon_{p,n,m+1}=\varepsilon_{p,n,m}+\Delta\varepsilon_{n,m+1}$$

b) If $\Delta\varepsilon_{n,m+1}\cdot\varepsilon_{e,n,m}>0$

$$\varepsilon_{e,n,m+1}=\varepsilon_{e,n,m}+\Delta\varepsilon_{n,m+1}$$
$$\varepsilon_{p,n,m+1}=\varepsilon_{p,n,m}\cdot$$

(8)

Thus the ground motion can be calculated by (3) in the elasto-plastic state and by (5) in the elastic state, respectively.

Next, the difference equations must be found to satisfy the boundary condition of the ground model. The boundary condition at the surface is that the shear stress is zero, i.e. $\sigma=0$. This can be solved by placing one hypothetic grid point above the surface as shown in Figure 4. Equating $U_{-1,m}$ to $U_{1,m}$ at any m, one finds that

$$\sigma=\frac{U_{-1,m}-U_{1,m}}{2\Delta x}\equiv 0 \qquad (9)$$

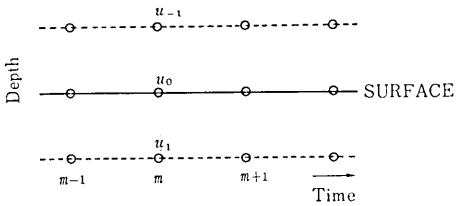

Fig. 4. Hypothetic grid points at ground surface.

is always satisfied. It should be noticed that perfect reflection of incident waves at the surface is automatically satisfied.

Concerning the boundary between the layers A and B, the soil material close to this boundary is assumed to remain in the elastic state. Actually only the soil close to the surface is expected to reach the nonlinear state.

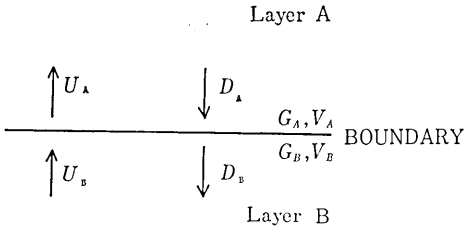

Fig. 5. Reflection and transmission of elastic waves at the boundary.

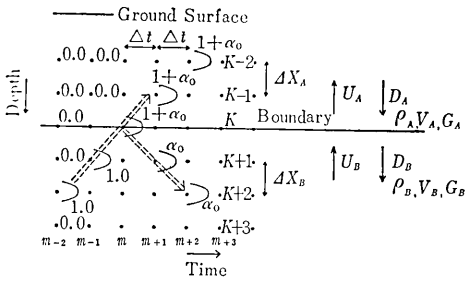

Fig. 6. Reflection and transmission of impulse at the boundary.

Then, the transmission and reflection law of elastic waves can be applied at this boundary. Note that the suffixes A and B are hereafter attached to the variables and constants associated with the layers A and B, respectively. Consider the case when the upward and downward waves approach the boundary simultaneously. The amplitudes of the waves are U_A and D_B, respectively. The amplitudes U_A of upward wave and U_B of downward wave through the boundary (Figure 5) are given by

$$\left.\begin{aligned} U_A &= \beta_0 U_B + \alpha^0 D_A \\ D_B &= \alpha_0 U_B + \beta^0 D_A \end{aligned}\right\} \tag{10}$$

where

$$\alpha_0 = \frac{1-k}{1+k}, \quad \beta_0 = 1+\alpha_0, \quad \alpha^0 = -\alpha_0, \quad \beta^0 = -\alpha_0, \quad k = \frac{G_B V_B}{G_A V_A}$$

in which α_0 is the coefficient of transmission and β_0 is the reflection coefficient for upward incident waves, while α^0 and β^0 are the transmission and the reflection coefficients for downward waves, respectively. Now consider the case when a unit impulse reaches the boundary from the side of layer B (Figure 6). At this boundary, the unit impulse is separated into two, namely the upward wave and downward wave. The amplitude U_A of the upward wave is obtained from (10) by

$$U_A = (1+\alpha_0) U_B . \tag{11}$$

The amplitude D_B of the downward wave is similarly given by

$$D_B = \alpha_0 U_B . \tag{12}$$

Next, consider the amplitude of an impulse at the boundary. First, in the upward wave of a unit impulse, equating the amplitude of the pulse to $1+\alpha^0$, (5) can be applied as it is, i.e.

$$\left.\begin{aligned} U_{k+1,m+1} &= U_{k,m} + U_{k+2,m} - U_{k+1,m-1} = \alpha_0 \\ &\quad\| \qquad\| \qquad\| \\ &\quad 1+\alpha_0 \quad 0 \qquad 1 \\ U_{k-1,m+1} &= U_{k-2,m} + U_{k,m} - U_{k-1,m-1} = 1+\alpha_0 \\ &\quad\| \qquad\| \qquad\| \\ &\quad 0 \quad 1+\alpha_0 \quad 0 \end{aligned}\right\} \tag{13}$$

In turn, in the case of the downward wave, the value of the amplitude at the boundary can be obtained by multiplying it by $1-\alpha_0$, i.e.

$$\left.\begin{aligned} U_{k+1,m+1} &= U_{k,m} + U_{k+2,m} - U_{k+1,m-1} = 1-\alpha_0 \\ &\quad\| \qquad\| \qquad\| \\ &\quad 1-\alpha_0 \quad 0 \qquad 0 \\ U_{k-1,m+1} &= U_{k-2,m} + U_{k,m} - U_{k-1,m-1} = -\alpha_0 \\ &\quad\| \qquad\| \qquad\| \\ &\quad 0 \quad 1-\alpha_0 \quad 1 \end{aligned}\right\} \tag{14}$$

So far, treatment of a unit impulse at the boundary is considered. For any form of waves, the value of the displacement $U_{k,m}$ at the boundary is obtained as follows

$$U_{k,m} = (1+\alpha_0)\,U_{k+1,m-1} + (1-\alpha_0)\,U_{k-1,m-1} - U_{k,m-2} \tag{15}$$

which is analogous to (13) and (14).

For layer B, the earthquake wave dissipating into the infinite half-space must be incorporated in the analysis. The co-ordinate system is chosen as shown in Figure 7. An input earthquake wave $F(m)$ is applied upward at the grid number n. As far as the displacement $U_{n-1,m-1}$ is concerned, it contains an upward wave and a downward wave. The downward wave should be subtracted in the analysis. As Figure 7 shows, the upward wave $\uparrow U_{n-1,m-1}$ in $U_{n-1,m-1}$ is equal to the input earthquake wave $F(m-2)$. Therefore the following holds.

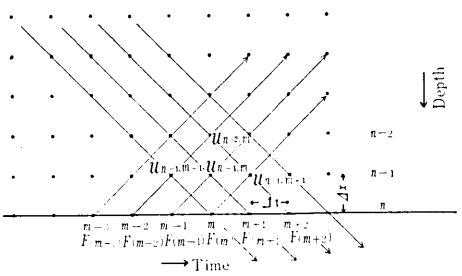

Fig. 7. Grid points of difference mesh.

$$\begin{aligned} U_{n-1,m-1} &= \uparrow U_{n-1,m-1} + \downarrow U_{n-1,m-2} \\ &= F(m-2) + \downarrow U_{n-1,m-1}\,. \end{aligned} \tag{16}$$

The displacement $U_{n-1,m+1}$ is expressed as

$$U_{n-1,m+1} = \uparrow U_{n-1,m+1} + \downarrow U_{n-1,m+1} \tag{17}$$

which is similar to (16). Also one can find that the following equation

holds.

$$\begin{aligned} U_{n-1,m+1} &= F(m) + \downarrow U_{n-1,m+1} \\ &= F(m) + \downarrow U_{n-2,m} . \end{aligned} \tag{18}$$

The displacement $U_{n-2,m}$ is given by

$$U_{n-2,m} = \uparrow U_{n-2,m} + \downarrow U_{n-2,m} . \tag{19}$$

Substitution of (19) into (18) leads to

$$U_{n-1,m+1} = U_{n-2,m} + F(m) - F(m-2) . \tag{20}$$

Thus the wave propagating downward in layer B is not reflected at the artificial boundary. Now the boundary conditions of this ground model are completely resolved in the difference equation.

4. Generation of simulated earthquake wave

From the results of analysis of many earthquake records, it has been found that an incident earthquake wave has a fairly constant velocity spectrum over a wide range of frequency. Autocorrelation of an earthquake motion generally decreases rapidly as the time interval becomes longer. This indicates that earthquake motions are indeterministic in nature. Since the frequency components of them are relatively invariant, the randomness of earthquake motions can be attributed to the randomness of phases of each frequency. Then, in simulating an earthquake motion, the following functions $g(t)$ having a constant velocity spectrum can be adopted as a first-step model.

$$g(t) = \sum_i \frac{b}{f_i} \cos 2\pi (f_i t + \phi_i) \tag{21}$$

where

b = velocity
f_i = frequency
t = time
ϕ_i = random variable distributed between 0 and 2π.

It is required, in generating (21) in a digital computer, that the following condition between earthquake duration time T and the frequency interval Δf must be satisfied by Someya-Shannon's Theorem.

$$\Delta f \leqq \frac{1}{2T} . \tag{22}$$

Since an earthquake wave is, in fact, transient, the stationary function given in (21) should be multiplied by the envelope function $\Phi(t)$, i.e.

$$f(t)=\Phi(t)\times g(t) \tag{23}$$

in which $\Phi(t)$ is assumed as follows.

$$\Phi(t)=\begin{cases}\exp(-1/t) & 0\leq t<3 \text{ sec}\\ 1 & 3<t\leq 12\\ \exp(-t+12) & 12<t\end{cases}$$

This function $f(t)$ is used in simulating an earthquake motion in a digital computer. The following two types of earthquake motions are synthesized: Model Wave No. 1 and Model Wave No. 2. In both waves the range of

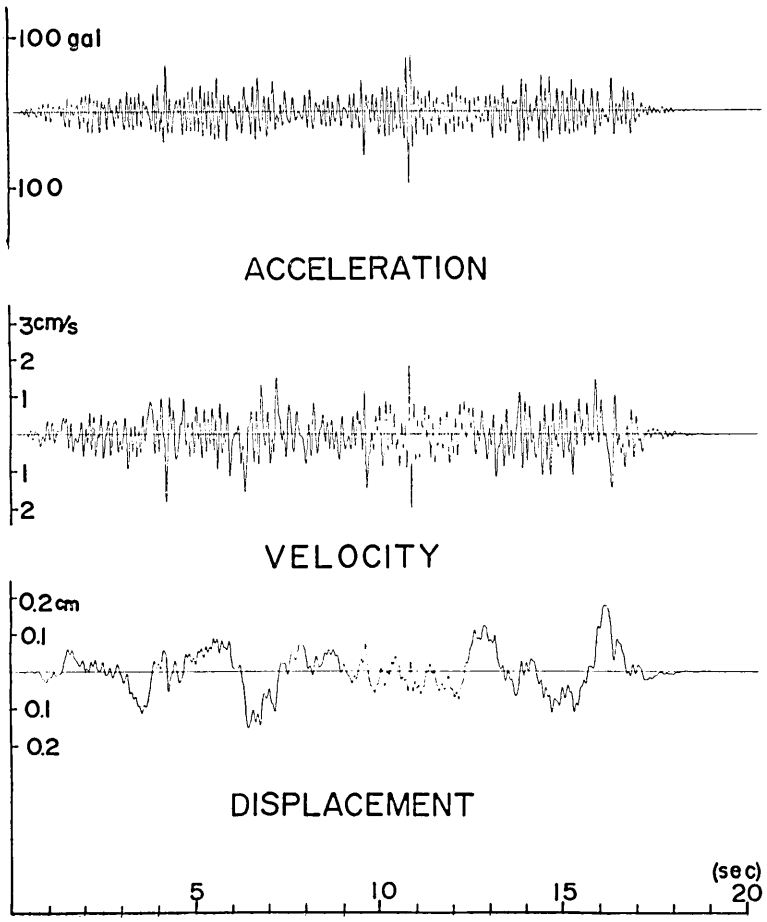

Fig. 8. Simulated earthquake wave No. 1.

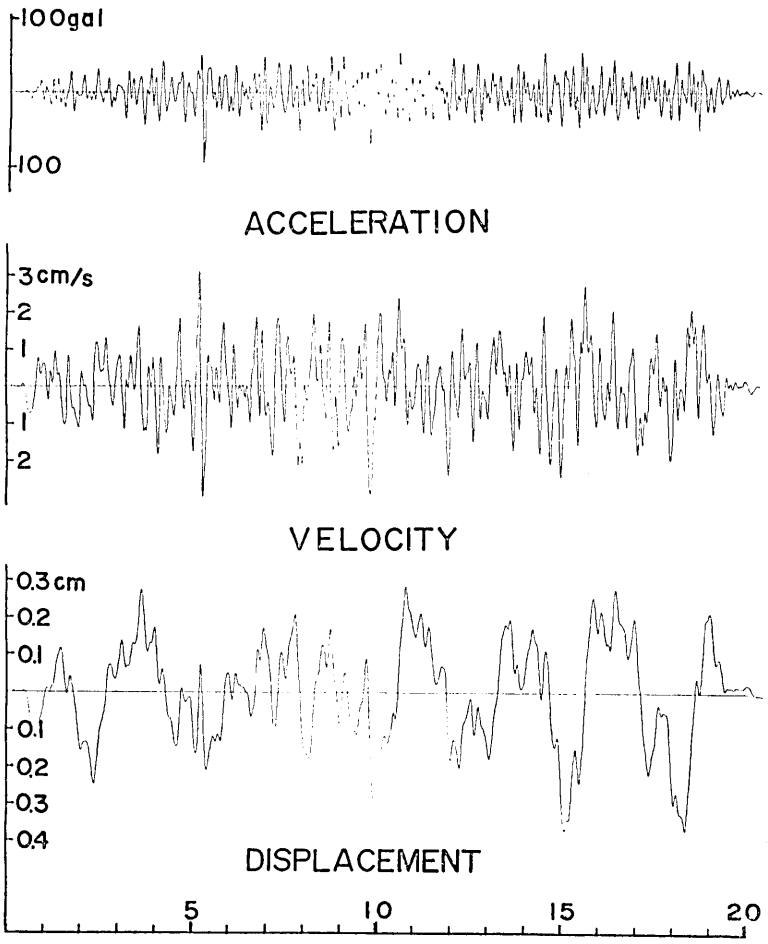

Fig. 9. Simulated earthquake wave No. 2.

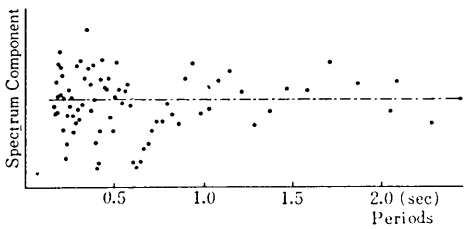

Fig. 10. Velocity spectrum of model wave No. 1.

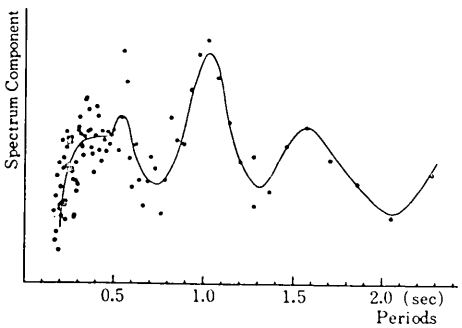

Fig. 11. Velocity spectrum of model wave No. 2.

frequency is between 0.25～10 Hz, with $\Delta f=0.025$ Hz, and the duration time is 20 sec., but they have different spectra. In Model Wave No. 1 the velocity spectrum is constant for all frequencies. On the other hand, in Model Wave No. 2 the frequency components above 3 Hz decrease at linearly. the velocity intensity at 10 Hz is 1/9 of that of 3 Hz. Model Waves No. 1 and 2 are shown in Figures 8 and 9. Comparing Model Wave No. 1 with No. 2, one finds that No. 2 has less high-frequency components, resulting in a slowly varying wave.

This can be confirmed from the results of Fourier spectral analysis as shown in Figures 10 and 11. Maximum acceleration of the waves is normalized to be 100 gal.

5. Assumption of parameter values used in the analysis

The values of the parameter used in the foregoing numerical example are:

shear wave velocity (surface layer A)	$V_A=100$ m/s
	$a=0.4$
(half-space B)	$V_B=300$ m/s
density of the soil for both layers	$\rho=2$ ton/m^3
elastic strain limit	$\varepsilon_a=0.001$
time interval	$\Delta t=0.005$ sec
grid point interval	$\Delta x=0.5$ m (layer A)
	1.5 m (layer B)
thickness of layer A	$H=20$ m (10 m, 7.5 m)

Besides the constant elastic strain limit, the case when the elastic strain limit increases linearly with depth is also considered in the numerical example. In this case, the elastic strain limit is specified to be 0.002 at a depth of 20 m from the surface. This is based on the conjecture that the elastic strain limit increases when lateral pressure becomes high.

6. Computational results

Nonlinear ground motions are investigated by the method described in 3.

(1) Response to stationary sinusoidal waves

The response at the surface is a sinusoidal wave for a stationary incident sinusoidal wave of a small amplitude. However, nonlinear response appears as the input amplitude increases. Figure 12 shows two example of nonlinear response at the surface subject to sinusoidal waves.

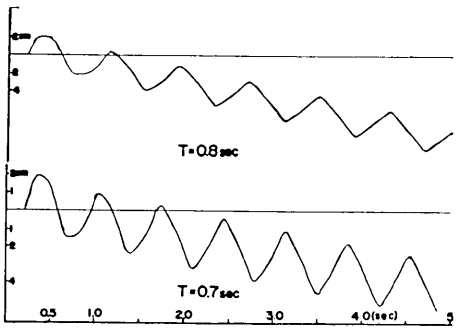

Fig. 12. Nolinear response to sinusoidal input wave.

The frequencies of the sinusoidal wave are close to the predominant period 0.8 sec. One can observe that the responses are deformed approximately into triangular shapes from sinusoidal shapes due to the nonlinearity. However, the amplitude of the responses varies little as time passes. The linear trend is caused by employing a bi-linear relation of stress and strain.

When a structure system subject to the excitation $f(t)$ is linear, response $y(t)$ can be determined by

$$y(t)=\int_0^t h(t-\tau)f(\tau)d\tau \tag{24}$$

in which the function $h(t)$ is the impulse response function of the system.

$$Y(i\omega)=H(i\omega)\cdot F(i\omega) \tag{25}$$

where

$$Y(i\omega)=\int_{-\infty}^{\infty} y(t)\ \exp\ (-i\omega t)dt$$

$$F(i\omega)=\int_{-\infty}^{\infty} f(t)\ \exp\ (-i\omega t)dt$$

$$H(i\omega)=\int_{-\infty}^{\infty} h(t)\ \exp\ (-i\omega)dt\,.$$

The function $H(i\omega)$ is the frequency transfer function. As far as the structure is linear, the frequency transfer function is invariant to any excitation. However, when the magnitude of the structural response is large, generally it becomes nonlinear due to the yielding of the structure. The variation of the frequency transfer function due to nonlinearity in case of a one-degree of freedom spring-mass system has been studied from various aspects (JENNINGS, 1968). The principal results of these studies are the elongation of the natural period and the increase of the apparent damping.

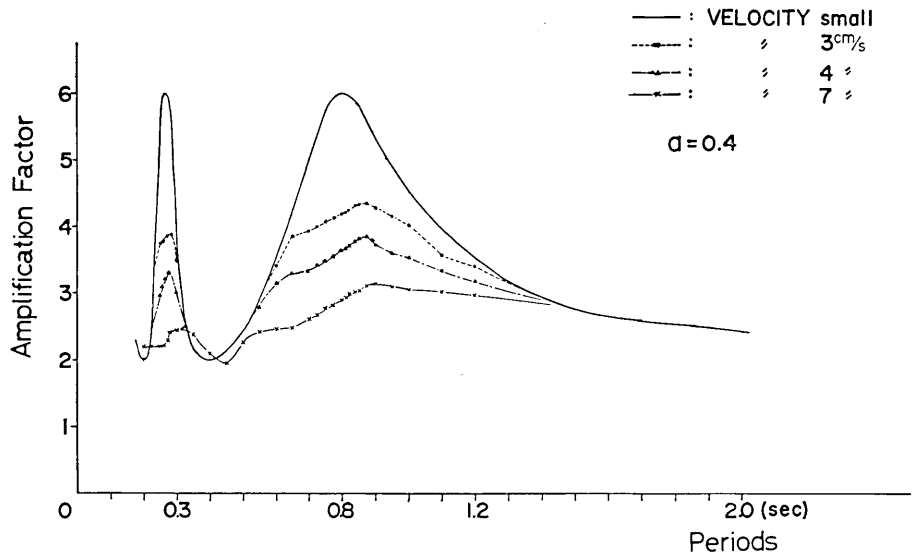

Fig. 13. Transfer functions of sinusoidal input wave.

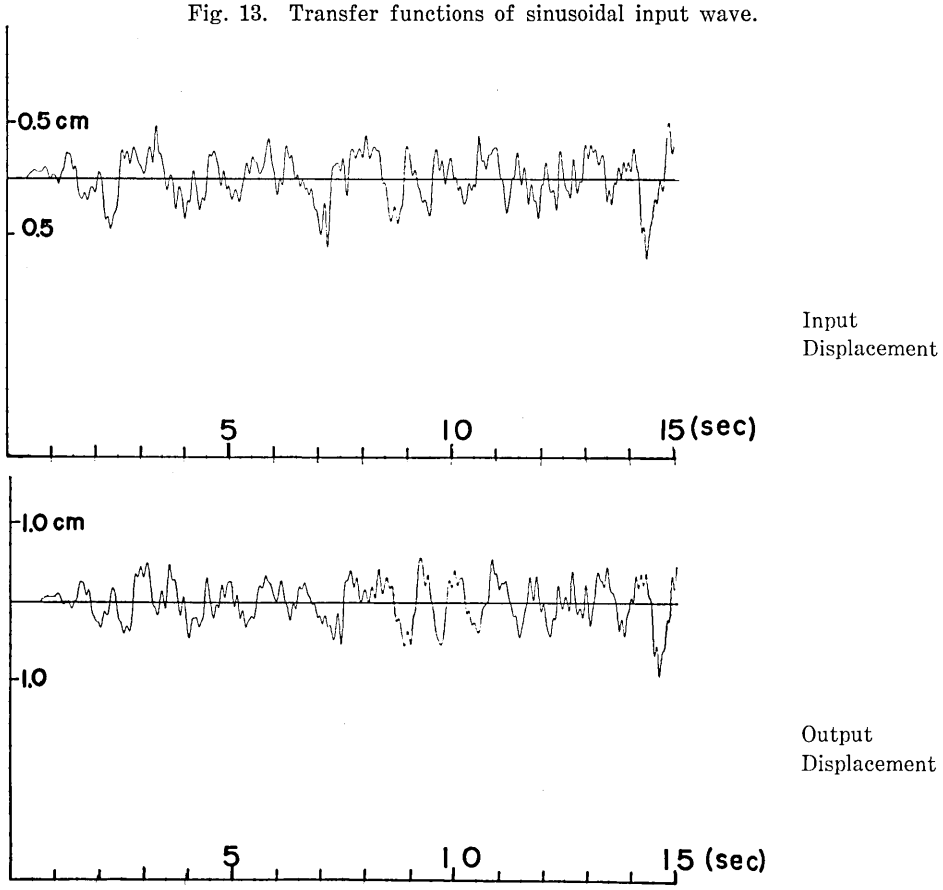

Fig. 14. Linear response at ground surface.

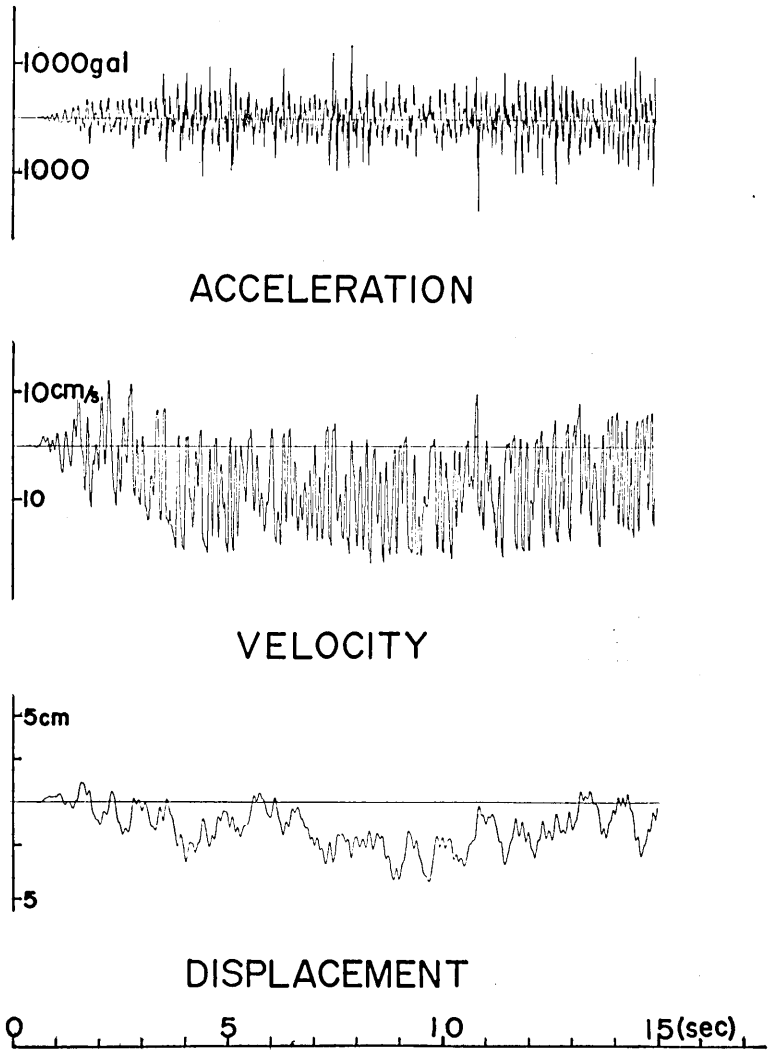

Fig. 15. Nonlinear response at ground surface.

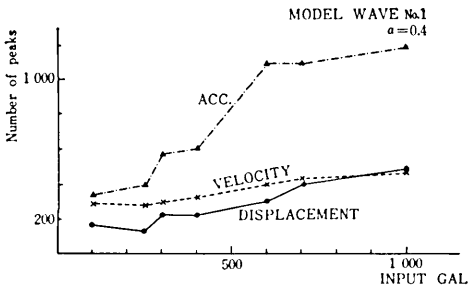

Fig. 16. Number of peaks of response.

Here, the frequency transfer function in the case of nonlinear ground motion resulting from sinusoidal waves is calculated by (25) in terms of the velocities of the input and output. Figure 13 indicates the calculated transfer function. The solid line shows the linear case. The first predominant

period is 0.8 sec., and the second one is 0.267 sec. and so on. It is remarkable that the amplification factor at the predominant period is only 6.0 even though internal damping of the soil material is neglected. In other words, the damping effect of dissipation of waves into an infinite half-space is considerable. As the input excitation becomes large, the apparent damping increases and the predominant period appears to be somewhat elongated.

(2) Response to earthquake waves

Figure 14 shows an example of the linear response at the surface. The response shape is rather similar to the input shape, which implies that the natural vibration is not strongly induced. This occurs because of the large dissipation damping as mentioned before. Next, Figure 15 shows an example of the nonlinear response. There is a long-period trend in the displacement response, but otherwisethe shape of the displacement response is almost identical to the linear one. However, the shapes of the velocity and acceleration are not so smooth as those in the linear response. This can be explained by increased high frequencies in the nonlinear response. Figure 16 shows the number of peaks in the displacement, velocity and acceleration surface responses for different magnitude of excitation of the same model wave. One can observe that the number of peaks, particularly in the acceleration, increases for larger excitation magnitude. It is widely accepted that, in nonlinear vibrations, the natural period is elongated and that the apparent damping increases. However, as far as nonlinear earthquake ground motion is concerned, the results shown in Figures 15 and 16 imply that this is not the case. From the

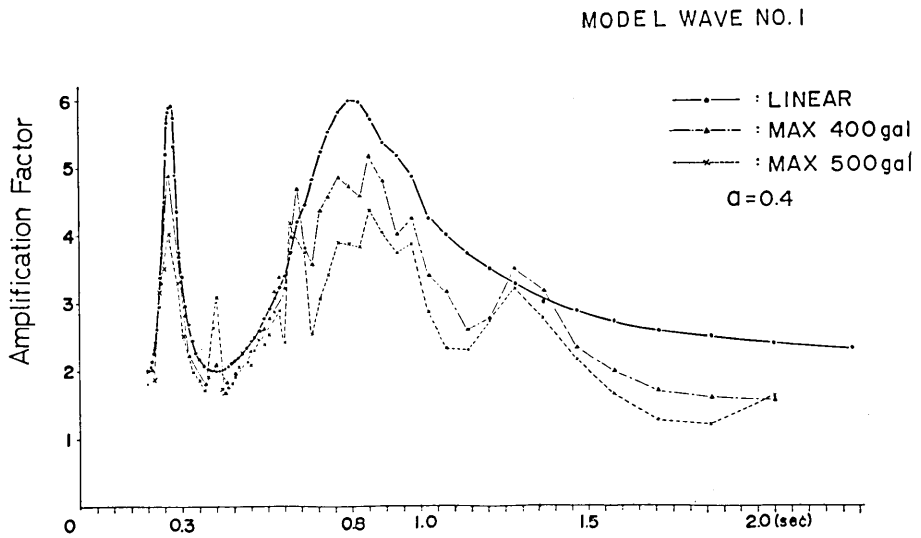

Fig. 17. Transfer functions.

velocity response shown in Figure 15, peak values are relatively constant throughout the response.

As mentioned in (1), in linear vibration, the frequency transfer function is inherent to the vibration system and is invariant to any input excitation. But, in nonlinear vibration, the frequency transfer function is dependent on the input excitation. It is of interest to know whether there is a great difference or not between sinusoidal and random inputs. Figure 17 shows

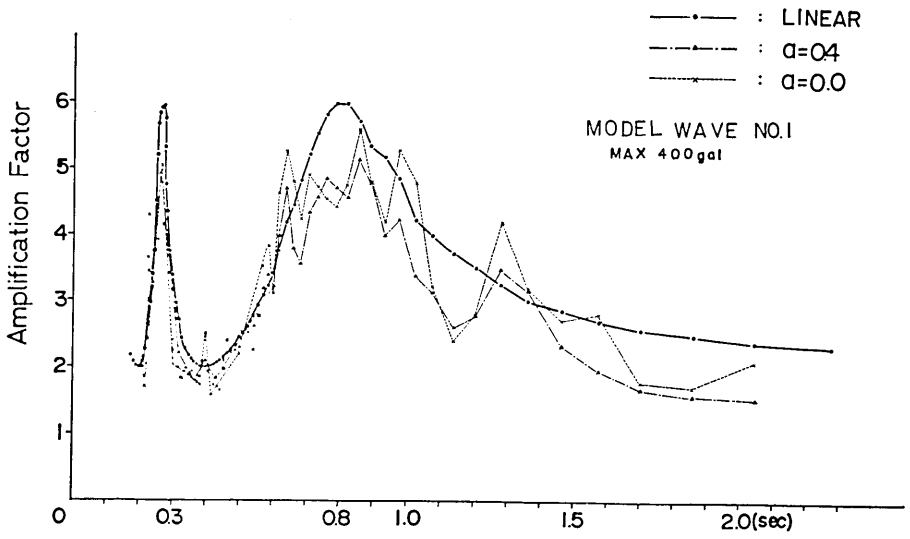

Fig. 18. Transfer functions.

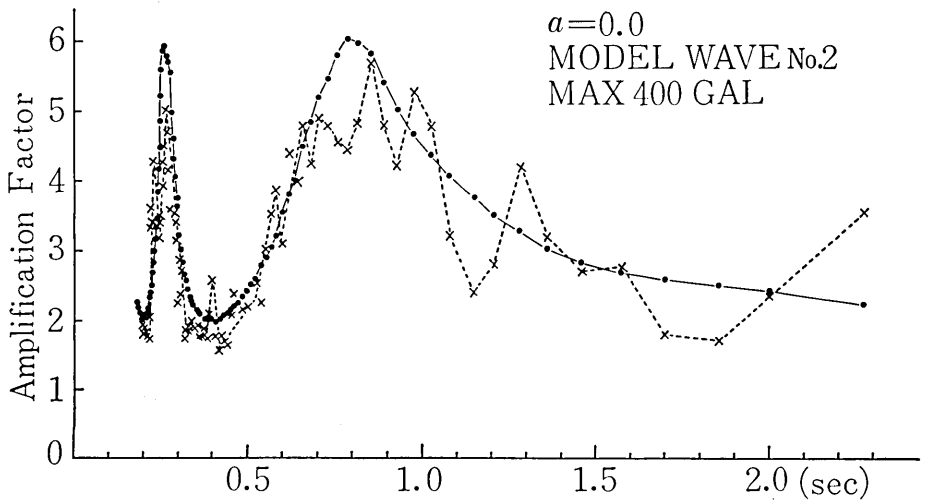

Fig. 19. Transfer functions.

the frequency transfer functions calculated in the case of Model Wave No. 1 input. It clearly indicates that the amplification factor decreases for larger input magnitude. Elongation of the natural period due to nonlinearity is not evident. It appears that the peak at the natural frequency is separated into a number of small peaks.

Figure 18 shows the frequency transfer functions in the case of the yielding coefficients $a=0.0$ and 0.4 for comparison. They are practically identical.

Figure 19 shows the frequency transfer functions in the case of Model Wave No. 2 input. They are similar to those in Figure 17.

Figures 20 and 21 show the frequency transfer functions when thicknesses of the surface layer are 10 and 7.5 m, respectively. They are also similar to those in Figure 17.

A decrease of the amplification factor and the disappearance of clear peaks at the predominant period in the nonlinear ground motions are found in Figures 17~21. HAKUNO et al. (1969) carried out an experimental study concerning the nonlinear response of steel structural members. On the other hand, this study is a theoretical study of nonlinear ground motion. Thus only qualitative comparison of the results of these two studies is allowed. The common results are:

a) The amplification factor in the nonlinear response is decreased.

b) Nonlinear response is not simply characterized by elongated natural period and increased apparent damping. Short period waves appear in the nonlinear response. The natural period is not clearly elongated and its peak is split into a number of small peaks.

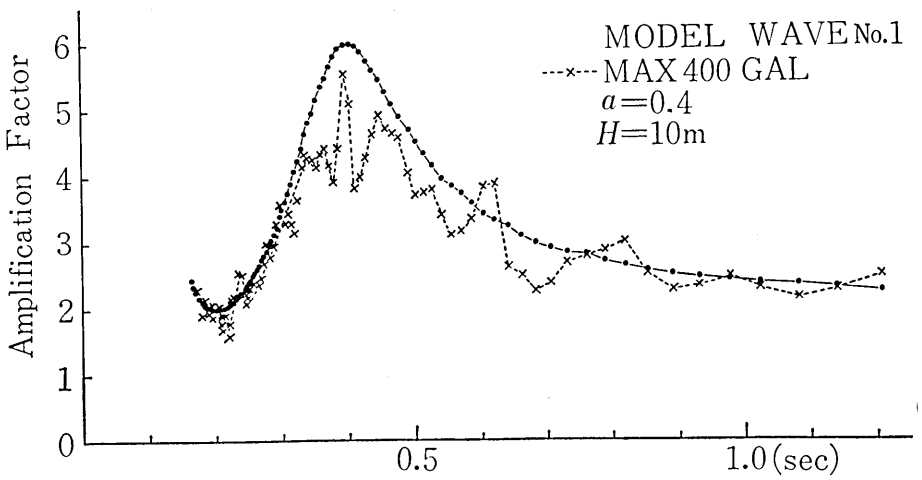

Fig. 20. Transfer functions.

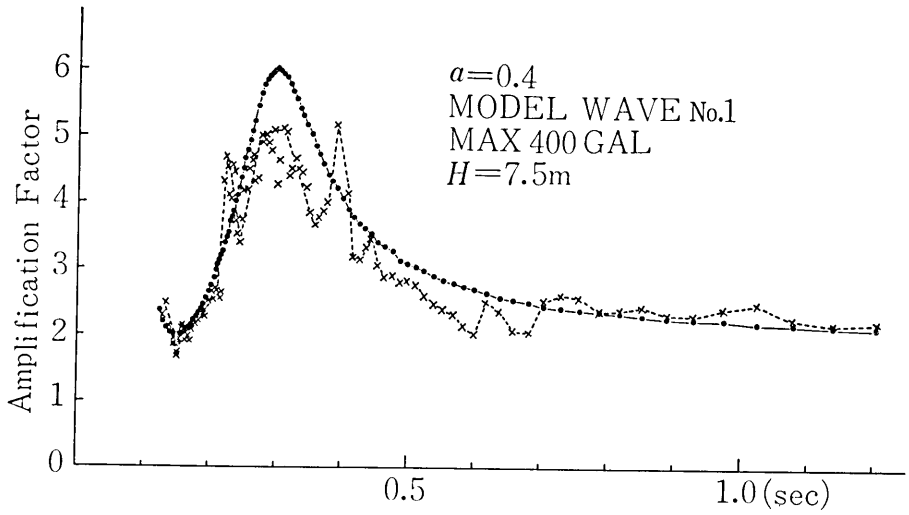

Fig. 21. Transfer functions.

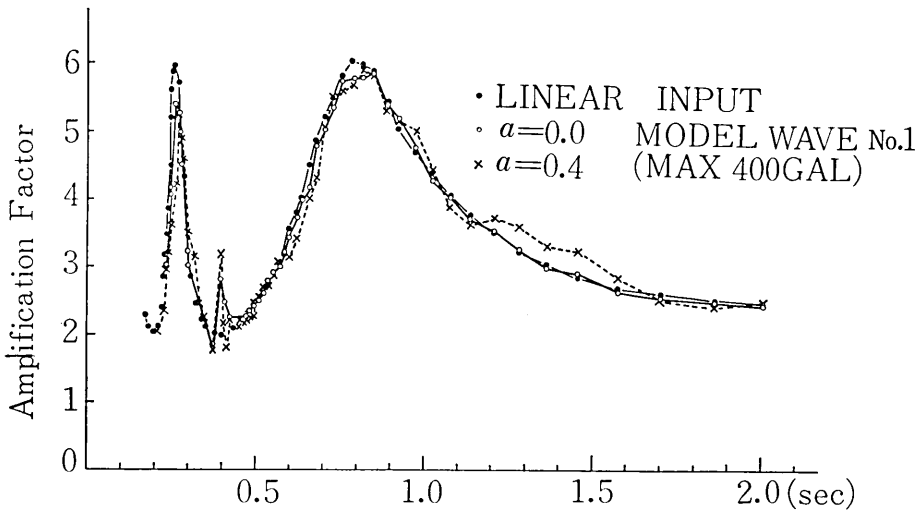

Fig. 22. Transfer functions.

Figure 22 shows the frequency transfer functions when the elastic strain limit in proportion to the depth. They differ little from each other since plastic strain in the soil hardly occurs under this situation.

7. Conclusions

The following can be concluded from this study:

i) In the elasto-plastic nonlinear ground motion subject to sinusoidal incident waves, the apparent damping increases and the predominant period

is somewhat elongated. In the case of random incident waves such as earthquake waves, however, only the apparent damping increases while the predominant period does not vary.

ii) Based upon i), it may be inappropriate to apply the equivalent linearization method to nonlinear ground motion due to an earthquake wave.

iii) In the surface layer subject to strong earthquake motion, the predominant period becomes undistinguishable and the surface ground motion tends to be a white noise.

8. Acknowledgement

The authors would like to express their thanks to Professor Shunzo Okamoto, President of Saitama University, for his valuable advice.

References

SEZAKI, K., and KANAI, K., 1932, Possibility of Free Oscillations of Strate excited by Seismic Waves. Part III, *Bull. Earthq. Res. Inst.*, **10**, 1-20.

IDRISS, I. M., and SEED, B. H., 1970, Seismic Response of Soil Deposits, *ASCE, Journal of the Soil and Foundation Engineering Division*, **97**, SM2, 631-638.

OKAMOTO, S., and HAKUNO, M., 1962, On the elasto-plastic vibration of the ground, *Proc. of Japan National Symposium on Earthquake Engineering*, 45-50.

JENNINGS, P. C., 1968, Equivalent Viscous Damping for Yielding Structures, *ASCE, Journal of the Engineering Mechanics Division*, **94**, EM4, 1003-1008.

HAKUNO, M., SHIDAWARA, M., and HARA, T., 1969, Dynamic Destructive Test of a Cantilever Beam, Controlled by Analog-Computer, *Proc. JSCE*, **171**, 1-9.

---

14. 地盤の非線形性を考慮した地震動の特性

筑波大学構造工学系 藤 野 陽 三
地 震 研 究 所 伯 野 元 彦

一般に，地盤の応力～ひずみ曲線は，ひずみ値が 10^{-4}～10^{-3} をこえると非線形性を示すことが知られている．通常，われわれの感じる震度 III, IV の地震では，地盤の最大ひずみは 10^{-3} をこえないか，こえてもごくわずかで線形として扱っても，それほど大差ないであろうとされている．しかし，震度 V をこえるような強い地震では，往々にして，地表の地盤が破壊することもあり，この場合には，当然線形領域をはるかにこえているものと思わざるを得ない．したがって，震度V以上の強い地震の場合には，地表軟弱層は破壊しないまでも，応力～ひずみ関係が非線形になっている可能性が強い．そのような強い地震動の性質は，過去の地震記録があれば，それを調べることにより，解明されると思われるが，現在のところほとんど得られていない．

本研究では，真下から地震波が入射して来る時，地表層が降伏した場合の地震動性状を適当なモデルによる数値シミュレーションにより解明しようとした．地表層のモデル化その他は以下のようにして行った．

1) 地表層のみが非線形の応力～ひずみ関係を持つものとして，それより下は無限に続く弾性体と

した．応力～ひずみ関係はバイリニア・ヒステリシスとした．

2) 地表層とその下の弾性体の間の地震波動の反射，屈折の関係は，弾性波のそれをそのまま適用する．

3) 方程式は差分化して解く．

数値シミュレーションの結果，次の事柄が知られた．

1) 従来言われて来た，「大地震になると地表層の卓越周期は長い方へ移動する」ということは疑問であって，卓越周期が移動するというよりも，増幅率が減って，卓越周期がばらばらになって，他の周期成分が現れて来る傾向が認められた．特に，全く別の長周期に小さいながらピークが出現する．

2) 1) の事柄から，地盤の非線形応答を取り扱うため，考えられている，ばね定数を小さくし，減衰定数を大きくして，非線形応答の近似を試みる等価線形化法には多くの疑問が生じる．